

PAPER • OPEN ACCESS

Research on Optimal Load Scheduling for Multiple Scenarios

To cite this article: Yifan Ding *et al* 2020 *J. Phys.: Conf. Ser.* **1639** 012060

View the [article online](#) for updates and enhancements.

You may also like

- [Partial discharge induced decomposition and by-products generation properties of HFO-1234ze\(E\)/CO₂: a new eco-friendly gas insulating medium](#)
Yi Li, Yifan Wang, Song Xiao et al.
- [The influence of flow separation mode on side-loads in a rocket nozzle](#)
Huawei Liu, Lin Zhang, Xinhua Yu et al.
- [Synergism in SF₆ mixtures with C=CC backbone compounds](#)
E A Egüz, J Pachin, H Vemulapalli et al.



ECS
The Electrochemical Society
Advancing solid state & electrochemical science & technology

DISCOVER
how sustainability intersects with electrochemistry & solid state science research

Research on Optimal Load Scheduling for Multiple Scenarios

Yifan Ding^{1*}, Molin Huo^{1,2}, Haiyan Jiang¹, Yahui Ma¹ and Aikang Chen¹

¹State Grid (Suzhou) City & Energy Research Institute Co., Ltd., Suzhou 215163, Jiangsu Province, China

²State Grid Energy Research Institute Co., Ltd., Beijing 102209, China

*dingyifan@sgeri.sgcc.com.cn

*Corresponding author's e-mail: dyifansea@163.com

Abstract. In recent years, the operation of power grid is under great pressure due to more and more distributed resources. This paper establishes three kinds of load models, namely the electric water heater(EWH), the electric vehicle(EV) and the energy storage(ES). The response cost, speed, capacity and duration are taken as the four characteristic elements to cluster the demand side loads. According to the scenario characteristics, the factor weights under different scenarios are determined. Furthermore, the particle swarm optimization (PSO) algorithm utilized to optimize the scheduling of demand-side resources selected by K-medoids clustering algorithm. Simulation results indicate that, by taking advantage of the complementarity of the time-domain and functional characteristics of multiple loads, the consumption needs of different scenarios can be satisfied.

1. Introduction

With the continuous acceleration of urbanization in China, the phenomenon of continuous and rapid growth of elastic loads, such as energy storages, electric vehicles and air-conditioners, is very prominent[1-2]. More and more distributed resources are constantly connected to the grid, so that the load side is beginning to be equipped with power characteristics[3-5]. It is increasingly difficult to balance supply and demand of power grid. Thus a more efficient regulation mechanism is necessary for power balance.

The research on demand response in foreign countries is not only limited to the implementation strategy, but also involved in the field of application design. Reference [6] proposes a predictive control scheme of the automatic demand response mechanism, which mainly takes the distributed resources connected to the power grid as the objects, supporting the large-scale implementation of demand response projects. Reference [7] proposes a demand response framework, which can be applied to the home LAN, as the hardware architecture connecting the Home Management System (HMS) and the device interface unit, to realize the home demand response function.

Demand response research in China starts relatively late. Reference [8] investigates the demand response behavior of some typical clients in a province. Through analysis of the survey, it is concluded that demand response behavior is mainly influenced by the characteristics of enterprise production, related incentives and prices. Reference [9] puts forward a refined model of thermodynamic controllable loads in the residential side. Effects of electricity price on the residential loads have been analyzed in detail. Reference [10] establishes an EV economic scheduling model based on demand



response, and realizes the purpose of transferring EV charging load through the optimization of EV charging price.

The practice and theory of demand response is rich in foreign countries, while domestic demand response is just beginning to develop. There is still a lack of research on the dispatch strategy for multiple loads. In this paper, the load models of EWH, EV and ES are constructed at first. Then a multi-scenario optimization scheduling strategy is put forward. Simulation results illustrate that, the proposed strategy is an ideal method for the load dispatch.

2. Load model construction

2.1. Electric Water Heater

2.1.1. Real-time reactive power calculating

The real-time reactive power of EWH can be calculated as follows:

$$Q = \sqrt{S^2 - (UI \cos \phi)^2} \quad (1)$$

$$S = UI \quad (2)$$

Where U is the voltage, I is the current, and $\cos \phi$ is the factor.

2.1.2. Response capacity and time calculating

1) In the standby state

The response capacity P_{DR} is served as

$$P_{DR} = P_X - P_Y \quad (3)$$

Which means the water heater changes its operation state from X to Y.

Accordingly, the calculating formation of the response time T_{DR} is

$$T_{DR} = \frac{c_{water} \times Vol \times (T_{set} - T_{real}) \times \rho_{water}}{P_Y} \quad (4)$$

Where c_{water} is the specific heat capacity of water; ρ_{water} is the density of water; Vol is the volume of the water heater; T_{set} and T_{real} are the given and real temperature respectively.

2) In the service state

The response capacity P_{DR} is similar to that in the standby state, while the response time T_{DR} is calculated as

$$T_{DR} = \frac{c_{water} \times Vol \times (T_{set} - T_{real}) \times \rho_{water} - \int_0^{T_{set}} c_{water} \times Q_{out} \times (T_{out} - T_{in}) \times \rho_{water} \times dt}{P_Y} \quad (5)$$

Where the temperature of EWH is constant when someone takes a bath.

2.2. Electric Vehicle

2.2.1. Real-time reactive power calculating

The real-time reactive power of EV can be calculated as in Equation (1).

2.2.2. Response capacity and time calculating

1) Charging scheduling

The response capacity P_{DR} is served as

$$P_{DR} = P_X - P_Y \tag{6}$$

Which means EV changes its operation state from X to Y.

Accordingly, the calculating formation of the response time T_{DR} is

$$T_{DR} = \begin{cases} Q(1 - SOC)/P_Y, P_X > P_Y \\ Q(1 - SOC)/P_X, P_X < P_Y \end{cases} \tag{7}$$

2) Discharging scheduling

The response capacity P_{DR} in the charging scheduling is the same as Equation (1).

Similar to Equation (7), the response time T_{DR} in the discharging scheduling is as in

$$T_{DR} = \begin{cases} Q(SOC - SOC_{low})/P_Y, P_X > P_Y \\ Q(SOC - SOC_{low})/P_X, P_X < P_Y \end{cases} \tag{8}$$

2.3. Energy Storage

2.3.1. Real-time reactive power calculating

The real-time reactive power of ES can be calculated as in Equation (1).

2.3.2. Response capacity and time calculating

1) Charging scheduling

The response capacity P_{DR} is served as

$$\begin{cases} 0 \leq P_{DR} \leq UI + S_N \cos \phi \text{ (Decreasing Situation)} \\ 0 \leq P_{DR} \leq S_N \cos \phi - UI \text{ (Increasing Situation)} \end{cases} \tag{9}$$

Where S_N is the rated power of the battery.

Accordingly, the calculating formation of the response time T_{DR} is

$$T_{DR} = \begin{cases} \frac{(1 - SOC) \times C \times SOH}{(UI - P_{DR}) \times q_{ch}}, P_{DR} \leq UI \text{ (Charging after decreasing capacity)} \\ \frac{(SOC - 1 + DOD_{max}) \times C \times SOH \times q_{dch}}{P_{DR} - UI}, P_{DR} \geq UI \text{ (Charging after decreasing capacity)} \\ \frac{(1 - SOC) \times C \times SOH}{(UI + P_{DR}) \times q_{ch}} \text{ (Increasing situation)} \end{cases} \tag{10}$$

2) Discharging scheduling

Different from Equation (9), the response capacity P_{DR} in the discharging situation is served as

$$\begin{cases} 0 \leq P_{DR} \leq S_N \cos \phi - UI \text{ (Decreasing Situation)} \\ 0 \leq P_{DR} \leq UI + S_N \cos \phi \text{ (Increasing Situation)} \end{cases} \tag{11}$$

Accordingly, the calculating formation of the response time T_{DR} is

$$T_{DR} = \begin{cases} \frac{(1 - SOC) \times C \times SOH}{(UI - P_{DR}) \times q_{ch}} \text{ (Increasing situation)} \\ \frac{(1 - SOC) \times C \times SOH}{(UI - P_{DR}) \times q_{ch}}, P_{DR} \leq UI \text{ (Charging after decreasing capacity)} \\ \frac{(SOC - 1 + DOD_{max}) \times C \times SOH \times q_{dch}}{P_{DR} - UI}, P_{DR} \geq UI \text{ (Charging after decreasing capacity)} \end{cases} \quad (12)$$

3. Multi-scenario optimization scheduling

3.1. Multi-scenario characteristic element analysis

There are primary considerations in different scenarios, while other elements are also important components of the strategy in specific cases. In order to quickly deal with different scenario characteristics and form a specific strategy scheme, it is necessary to match different characteristic element and scenarios. Then different weight schemes and demand response strategies are formed.

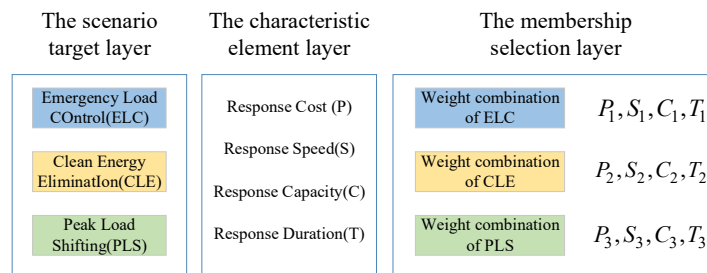


Figure 1. Schematic diagram of characteristic elements analysis.

There are four factors taken into consideration in this strategy, namely response cost, response speed, response capacity and response duration. The average value is taken as the benchmark, then the ratio of an element to the average value is calculated as the weight of the specific element.

The scenarios of peak load shifting, emergency load control and clean energy consumption are identified with a, b and c respectively. Set response cost, response speed, response capacity and response duration with P, S, C, T to describe the average of the four elements under each scenario. $P_a, S_a, C_a,$ and T_a represent the mean under the peak load shifting scenario, and so on. p_x, s_x, c_x and t_x represent the actual value of the x-th load, and n is the total number of loads, and m is the number of scenarios.

The calculation process is explained with an emergency load control scenario.

- Calculate the average of an element in an emergency load control scenario.

$$P_b = \sum_x^n p_x / n \quad (13)$$

- Calculate the average of an element under all scenarios.

$$\bar{P} = \sum_m P_{a/b/c} / m \quad (14)$$

- Calculate the factor ratio Q of the emergency load control scenario relative to all scenarios.

$$Q_{bP} = \bar{P}_b / \bar{P} \quad (15)$$

- The ratio of other elements in the emergency load control scenario can be obtained by the same method.

$$Q_{bS} = \frac{S_b}{S} = \frac{\sum_x^n S_x / n}{\sum_m S_{a/b/c} / m} \tag{16}$$

$$Q_{bC} = \frac{C_b}{C} = \frac{\sum_x^n C_x / n}{\sum_m C_{a/b/c} / m} \tag{17}$$

$$Q_{bT} = \frac{T_b}{T} = \frac{\sum_x^n t_x / n}{\sum_m T_{a/b/c} / m} \tag{18}$$

- Comparing the factor ratios of Q_{bP} , Q_{bS} , Q_{bC} and Q_{bT} , the maximum value is taken as the primary consideration of the scenario.
- The same is true for other scenarios.

3.2. Demand-side resource clustering analysis

The Grasshopper optimization algorithm is taken for the short-term prediction. Based on historical data accumulation, the data of the cost, speed, capacity and duration in the expected response are predicted for each scenario element. Then, the demand side resources are clustered by K-medoids algorithm. Selecting Euclidean distance as a cluster similarity indicator, part of load data clustering process is as follows.

- Initialize the cluster center. The load data set D_s is composed of n eigenvectors, represented as $D_s = \{D_1, D_2, \dots, D_n\}$. Randomly K vectors are selected as the initial cluster centers $C_C = \{C_{c1}, C_{c2}, \dots, C_{cn}\}$.
- Cluster division. All load eigenvectors are divided to each cluster center according to the nearest Euclidean distance. The distance ED between D_i and C_{ck} is calculated as

$$ED = \sqrt{\sum_{i=1}^T (D_i - C_{ck})^2} \tag{19}$$

Where T is the characteristic vector dimension of the time-series load.

- Updating the cluster center. In various clusters, the sum of distances of each load eigenvector to other data vectors of the current cluster are calculated according to Equation (19), and the distance and the minimum load data vector are selected as the new cluster center.

$$SD = \sum_{j=1}^J ED_{D_{i,j}} \tag{20}$$

Where $ED_{D_{i,j}}$ is the distance of D_i and D_j , J represents the number of eigenvector for the cluster D_i , and SD is the sum of the distance from D_i to all vectors in the current cluster.

In this section, multiple types of elastic loads are taken into consideration. As users have different utilization frequency and dependence on the three types of loads, these loads can be set for reasonable response levels according to their own power consumption rules and preferences. Three colors are used to indicate the order of response, while green, yellow and red load groups respond in turn.

In this DR policy, the aggregator needs to determine the response order of the devices in the same color group based on the weighted factor E , which is arranged from small to large.

$$E = \alpha A + (1 - \alpha) B \tag{21}$$

Where A is the times of scheduling loads, α is the weight coefficient, and B is the status value for different elastic load devices. A is to be calculated as

$$A = \begin{cases} \frac{|TE_{L,now} - TE_{L,set}|}{\Delta TE_L}, \forall L \in WH \\ \frac{|EN_{L,now} - EN_{L,target}|}{|TI_{L,now} - TI_{L,target}|}, \forall L \in EV \\ \frac{|EN_{L,now} - EN_{L,total}|}{EN_{L,total}}, \forall L \in ES \end{cases} \quad (22)$$

Where $TE_{L,now}$ and $TE_{L,set}$ are the current and set temperatures of the load L respectively; ΔTE_L is the temperature demand range the load L ; $EN_{L,now}$ and $EN_{L,target}$ are the current and target electricity of the load L respectively; $TI_{L,now}$ and $TI_{L,target}$ are the current and target travelling time of the load L respectively; $EN_{L,now}$ and $EN_{L,total}$ are the current and total capacity of the load L respectively.

The elastic loads governed by the aggregator respond in order of the green, yellow and red group. For the peak load shifting scenario, loads with a smaller E value in the same group are given a priority to respond.

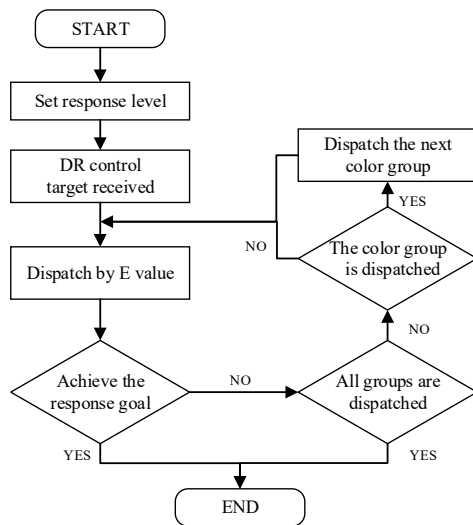


Figure 2. Process of multiple loads dispatch based on grouping.

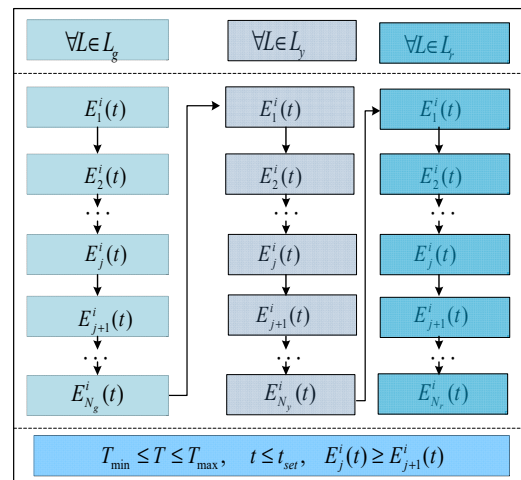


Figure 3. The execution sequence of multiple loads dispatch.

It is assumed that within the scope of the aggregator, the red user group includes N_r elastic load, while the yellow and green user groups include N_y and N_g elastic loads respectively. The execution order of regulation by E is shown in figure 3.

The first layer in the above figure is the color group of the elastic load. The middle layer is the load control sequence within each color group. The bottom layer is the control constraint for multi types of elastic load. $E_j^i(t)$ represents the weighted coefficient value of the j -th load that belongs to the i -th aggregator at the t -time. L_r , L_g and L_y are respectively the elastic load sets of the red, green and yellow group. T_{min} and T_{max} respectively indicate the upper and lower limits of the temperature controlled load dead zone. t_{set} is the time limit for EV.

3.3. Multi-scenario demand side resource regulation strategy construction

To further illustrate demand-side resource regulation strategies suitable for multiple scenarios, it is necessary to analyze characteristic elements in different scenarios before load scheduling. Based on different scenarios, the non-characteristic elements are divided into characteristic target elements and constraint elements. Furthermore, the PSO multi-objective algorithm is used to optimize the scheduling of demand-side resources selected by clustering[11]. The specific process of the demand side resource scheduling strategy is shown in the figure.

Take the emergency load control scenario as an example. Through the collection, analysis and processing of historical data, suppose that the characteristic affiliation of the emergency load control scenario has been determined to be the response speed, while the response capacity and cost are characteristic target elements and the response duration is the characteristic constraint element. Firstly, the demand side resources are clustered according to the response speed, so that the fastest response load group is met for requirements of the emergency load control scenario. Then, with the response cost and capacity as objective functions and the response time as constraints, the PSO multi-objective optimization algorithm is used to obtain the non-inferior solution set of load group satisfying the requirements.

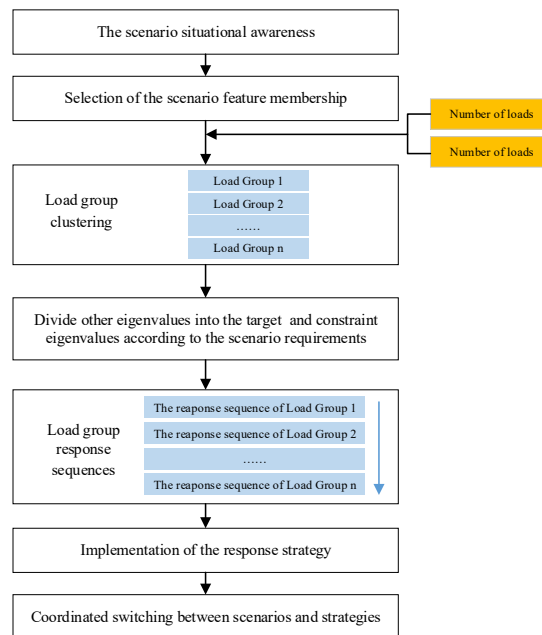


Figure 4. Demand-side resource scheduling flow chart.

When scheduling demand-side resources, the constraint eigenvalues of the scenario are used to cluster the demand-side resources, so as to obtain load groups satisfying the requirements of different scenarios. In order to further satisfy the scheduling order of the demand side resource, the priority of the demand side resource is determined by the target eigenvalues of different scenarios.

$$M_{x,i} = k_1\alpha_1 \left(\frac{p_{\max} - p_i}{p_{\max} - p_{\min}} \right) + k_2\alpha_2 \left(\frac{s_{\max} - s_i}{s_{\max} - s_{\min}} \right) + k_3\alpha_3 \left(\frac{c_{\max} - c_i}{c_{\max} - c_{\min}} \right) + k_4\alpha_4 \left(\frac{t_i}{t_e - t_s} \right) \quad (23)$$

Where k_1, k_2, k_3 and k_4 are Booleans, which indicate the eigenvalue type; p_i, s_i, c_i and t_i indicate the eigenvalues of the i -th load itself; p_{\max} and p_{\min} are the maximum and minimum response cost in the load group; s_{\max} and s_{\min} are the maximum and minimum response speed in the load group; c_{\max} and c_{\min} are the maximum and minimum response capacity in the load group; t_e and

t_s are the start and end time of scheduling; $\alpha_1, \alpha_2, \alpha_3$ and α_4 represent the weight of various eigenvalues in different scenarios, while $\sum \alpha=1$.

The values of $M_{x,i}$ in the load group are compared to form the response sequence, as shown in figure 5. Different proportional coefficients correspond to different strategies. The response strategy library is established with different regulatory sequences in the load groups.

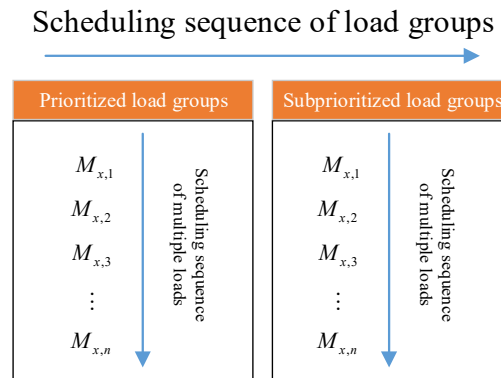


Figure 5. Schematic diagram of scheduling sequence.

4. Case study

4.1. Case introduction

In view of the demand-side resource scheduling strategy for multi-scenarios proposed in the previous section, the PSO multi-objective optimization algorithm is utilized for simulation to verify the validity of the proposed strategy in this section. Firstly, it is necessary to set the algorithm parameters, including the population size M , the dimension N , the iterative step N and other information. Secondly, the position x and velocity v of the particles have to be initialized. Then the individual fitness is calculated according to the fitness formula. Furthermore, the PSO update module updates the individual optimal particle according to the new particle location. Finally, the non-inferior solution set update module screenings non-inferior solutions according to the new particle dominance relationship. The position and velocity update formulas are shown as below.

$$\begin{cases} v^{k+1} = wv^k + c_1r_1(p_{id}^k - x^k) + c_2r_2(p_{gd}^k - x^k) \\ x^{k+1} = x^k + v^k \end{cases} \quad (24)$$

Where w is the inertia factor to readjust the global and local seeking performance; c_1 and c_2 are constants and usually set to 2, but not necessarily 2; r_1 and r_2 are random numbers on the interval $[0,1]$.

In this section, three typical loads of EWHs, EVs and ESs are simulated in matlab2017 to verify the proposed strategy above.

Table 1. Simulation parameter setting

Load Type	Number	The Optimal Range of The Load State	Charge/Discharge Power (W)
EWH	400	22°C~30°C	1000~5000
EV	200	Full	4000
ES	300	—	3000

4.2. Analysis of the scheduling effect of elastic loads

Figure 6 shows the corresponding contrast of the effect before and after demand response. It can be seen that the load joint scheduling curve coincides completely with the elimination target curve, while all three kinds of loads have been involved in regulation. But when a single type of load is invoked, such as EWHs or EVs, the combined adjustment effect is not achieved. This is due to the time-domain and functional characteristics of EWHs or EVs. EWH will be forced to charge when it is below 22°C, and will be forced to disconnect when it is above 30°C. EVs are constrained by the arrival and departure time. On the other hand, while the remaining stay time of EVs is less than the charging time, EVs have to be forced charging to ensure that EVs reach the desired state when leaving. These characteristics of EWH and EV will make it difficult to reach or far exceed the target amount of consumption in some period. However, a high level of matched consumption can be achieved by taking advantage of the complementarity of time-domain characteristics and functional characteristics of multiple types of loads.

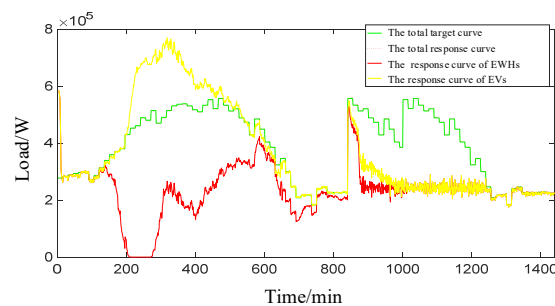


Figure 6. Results of elastic loads scheduling.

4.3. Analysis of state changes in the scheduling process of multiple loads

The temperature changes of 400 EWHs in a day is illustrated in Figure 7. EWHs fluctuates continuously between 22°C and 30°C. During 200~300min, numbers of EWHs with high temperature have to be powered off, while EVs are charging centrally with a high level of load consumption. During 700~800min, only part of EWHs with high temperature turn off due to little amount of demand response requirement. Figure 8 shows the changes in the charged state of 200 EVs. Due to the long charging time and short residence time of EVs, a large number of EVs are charged centrally within 200~400min. The changes in the charged state of 300 ESs are indicated in Figure 9. In the early stage, the load demand is much larger than the target amount, which requires ESs to discharge. In the later stage, the charging load demand is small, so ESs are required to carry out charging operation to achieve the goal of matching the final load consumption with the target consumption.

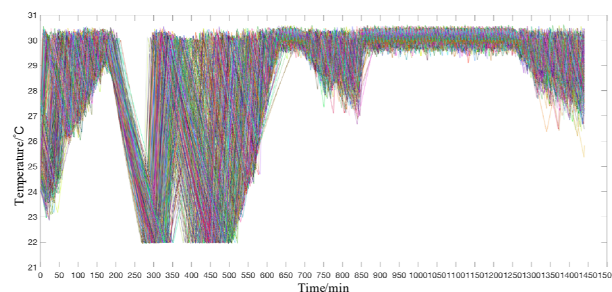


Figure 7. The temperature changes of EWHs within a day.

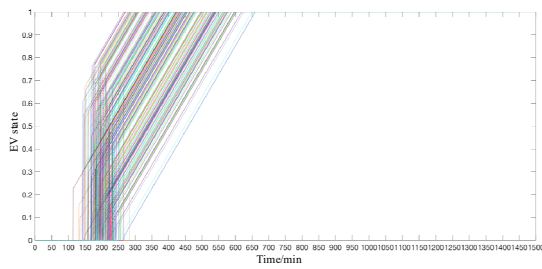


Figure 8. Charging curves of EVs.

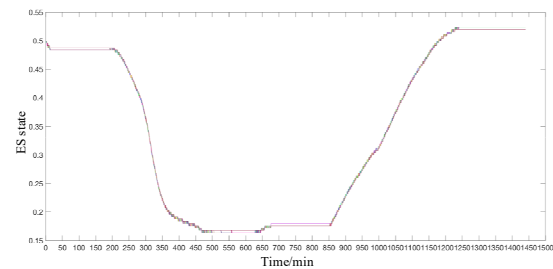


Figure 9. The state curves of ESs within a day.

4.4. Analysis of demand-side resource scheduling

Figure 10 shows the number of loads among demand-side resources that can be dispatched in 590-620 minutes in a day. These three types of elastic loads can be seen as scheduled ones, such as EWH whose water temperature is less than 30°C and higher than 22°C, EV whose charged state is less than the expected state during the stay, ES with charged state between 0 and 1.

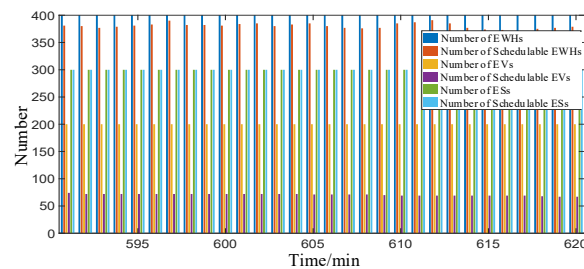


Figure 10. Demand side resource scheduling situation for local periods.

5. Conclusion

In this paper, models of EWH, EV and ES are constructed respectively. The response characteristics of various loads are taken into consideration in each model. In order to satisfy the load scheduling requirements under different scenarios, the four characteristic indicators are established to characterize each scenario. K-medoids algorithm is utilized to cluster the demand side resources. Then the target eigenvalues of different scenarios are applied to determine the priority of the demand side resources. By adjusting the proportional coefficient of eigenvalues, the response strategy library is established with different regulatory sequences in the load groups. The results show that, it is difficult to match the target load curve with the actual load curve in a single type of load scheduling, while a high level of matched consumption can be achieved by taking advantage of all three kinds of loads.

Acknowledgments

This paper is supported by National Natural Science Foundation (No. U1766212) and National Key Research and Development Project (No. 2017YFE0101800).

References

- [1] Conejo A J, Morales J M, Baringo L. (2010) Real-time demand response model. *IEEE Transactions on Smart Grid*, 1:236-242.
- [2] Soares J, Morais H, Sousa T, et al. (2013) Day-ahead resource scheduling including demand response for electric vehicles. *IEEE Transactions on Smart Grid*, 4:596-605.
- [3] Hassanniakhebari M, Hosseini S H, Soleymani S. (2020) Demand response programs maximum participation aiming to reduce negative effects on distribution networks. *International Transactions on Electrical Energy Systems*, 3.

- [4] Lu R, Hong S H, Yu M. (2019) Demand Response for Home Energy Management Using Reinforcement Learning and Artificial Neural Network. *IEEE Transactions on Smart Grid*, 10:6629-6639.
- [5] Singh V P, Samuel P, Kishor N. (2016) Impact of demand response for frequency regulation in two-area thermal power system. *International Transactions on Electrical Energy Systems*, 27:1-23.
- [6] Ioannis Lampropoulos, Paul P.J.van den Bosch and Wil L.Kling. (2012) A Predictive Control Scheme for Automated Demand Response Mechanisms. In: 2012 3rd IEEE PES Innovation Smart Grid Technologies Europe.
- [7] M.Pipattanasomporn, M.Kuzlu, S.Rahman, (2012) Demand Response Implementation in a Home Area Network: A Conceptual Hardware Architecture. In: *Innovative Smart Grid Technologies*.
- [8] Zhang C,Wang B and Li Y. (2012) Demand response behavior of typical industrial users. *East China Electric Power*, 40:1701-1705.
- [9] Zhao H, Liu G, Jia H, et al. (2014) Analysis of demand response program based on refined models,” *Power System Protection and Control*, 42: 62-69.
- [10] Pan Zi, Gao C. (2015) Economic dispatch of electric vehicles based on demand response,” *Electric Power Construction*, 36:139-145.
- [11] Thongchart K, Yaser Q, and Yasunori M. (2016) “Optimum battery energy storage system using PSO considering dynamic demand response for microgrids. *International Journal of Electrical Power & Energy Systems*, 83:58-66.